water

MDPI

Article

Effects of Geosynthetic Reinforcement on Tailings Accumulation Dams

Changbo Du [1,*], Lidong Liang [1], Fu Yi [2] and Ben Niu [1]

[1] School of Civil Engineering, Liaoning Technical University, Fuxin 123000, China; LLD18342847093520@163.com (L.L.); niu18535527973@163.com (B.N.)
[2] College of Architecture and Transportation, Liaoning Technical University, Fuxin 123000, China; yifu9716@163.com
* Correspondence: duchangbo2839@163.com

Abstract: Owing to the complexity of current reinforcement mechanisms, test results from existing models alone cannot provide a basis for the design of new tailings dam reinforcement projects. On-site reinforced tailings accumulation dam testing is thus required to further understand the reinforcement mechanism. In this study, the influence of reinforcement on tailings dams and the variation law of pore water pressure (PWP) and internal pressure (IP) in the dam body after slurry discharge were analysed, and a comparative analysis was performed. The results showed that during the field test, the PWP and internal earth pressure of the accumulation dam after grouting gradually increased over time. Reinforcement can greatly reduce the PWP and IP of the reinforced dam; compared with geotextiles, the reinforcement effect of geogrids is slightly greater. Based on these results, we conclude that geosynthetics are a good choice for strengthening tailings accumulation dams.

Keywords: polymer; composite material; mechanism

Citation: Du, C.; Liang, L.; Yi, F.; Niu, B. Effects of Geosynthetic Reinforcement on Tailings Accumulation Dams. *Water* **2021**, *13*, 2986. https://doi.org/10.3390/w13212986

Academic Editors: Xiaoli Liu, Jiangshan Li and Shuguang Zhang

Received: 3 September 2021
Accepted: 19 October 2021
Published: 22 October 2021

1. Introduction

Tailings ponds, structures built to store mine tailings, represent the largest hazard source of a mine. Improving the stability of tailings accumulation dams is a significant concern because their operation is not only related to the smooth progress of mine production and construction but also to the safety of lives and property downstream of the dam and in the surrounding environment [1–5].

It is well known that new geosynthetic materials can improve soil structure and strength, as they have been widely used for strengthening in subgrade and slope engineering [6–9]. Given that the reinforcement of a tailings dam is similar to that of subgrade and slope engineering, geosynthetics have been considered for this application [10–14]. Model testing, an important means of engineering and scientific research, can be employed to obtain regular or qualitative conclusions regarding the research object and has been widely used in many fields [15]. Several scholars have contributed significantly to indoor model test research on reinforced foundations and have drawn useful conclusions [16,17]. For instance, Yin et al. [18] designed a tailings accumulation dam model based on the Longdu tailings pond and conducted a failure model test of a reinforced accumulation dam, specifically testing the effects of dam reinforcement and different failure modes. Jing et al. [19] conducted an overtopping failure model test of a tailings pond dam and found that reinforcement can effectively reduce the overtopping failure of tailings pond flooding. Matsuoka et al. [20] proposed a new geobag technology for strengthening slopes and foundations and studied its reinforcement mechanism, engineering characteristics, and design method. The stress mechanism, deformation law, and stability of reinforced tailings dams are not only related to the properties and layout of the reinforced materials but also to the properties of the tailings, construction technology, environment, and other factors. However, model tests cannot fully simulate the specific construction methods

and environmental impact on the site [21–23]. Owing to the complexity of reinforcement mechanisms, existing test results cannot provide a design basis for all reinforced tailings projects. Thus, on-site testing is required for further understanding of the applied reinforcement mechanism.

Through field prototype tests of three different types of tailings accumulation dams (conventional, geogrid-reinforced, and geotextile-reinforced), the influence of reinforcement on the tailings dam and the variation law of pore pressure and IP in the dam body after slurry discharge were analysed. Additionally, data from the three types of test dams were compared and analysed. The reinforcement effect and action mechanism of the dam body after reinforcement were also explored and tested.

2. Design of the Field Test Scheme

To study the stress, deformation, and working performance of a reinforced tailings dam, a field test of geosynthetic-reinforced tailings dams was conducted at the No. 5 auxiliary dam of the Fengshuigou tailings pond in the Qidashan concentrator of the Liaoning Angang mining group in China (see Figure 1).

Figure 1. Site test location.

2.1. Site Damming Design Scheme

The side length of the specific test area was approximately 15 m. A shallow pit of approximately 1 m was excavated in the test area, and 4 m-high surrounding accumulation dams were built. The surrounding accumulation dams were designated as (a), (b), (c), and (d). The accumulation dam (b) was designed as a conventional accumulation dam. The accumulation dams (a) and (c) were designed to be piled with geogrid and geotextile, respectively. The accumulation dam (d) was designed as an auxiliary dam and was not involved in this analysis. The design of the surrounding tailings accumulation dams is depicted in Figure 2; see Table 1 for the specific accumulation type and laying parameters of the first three accumulation dams.

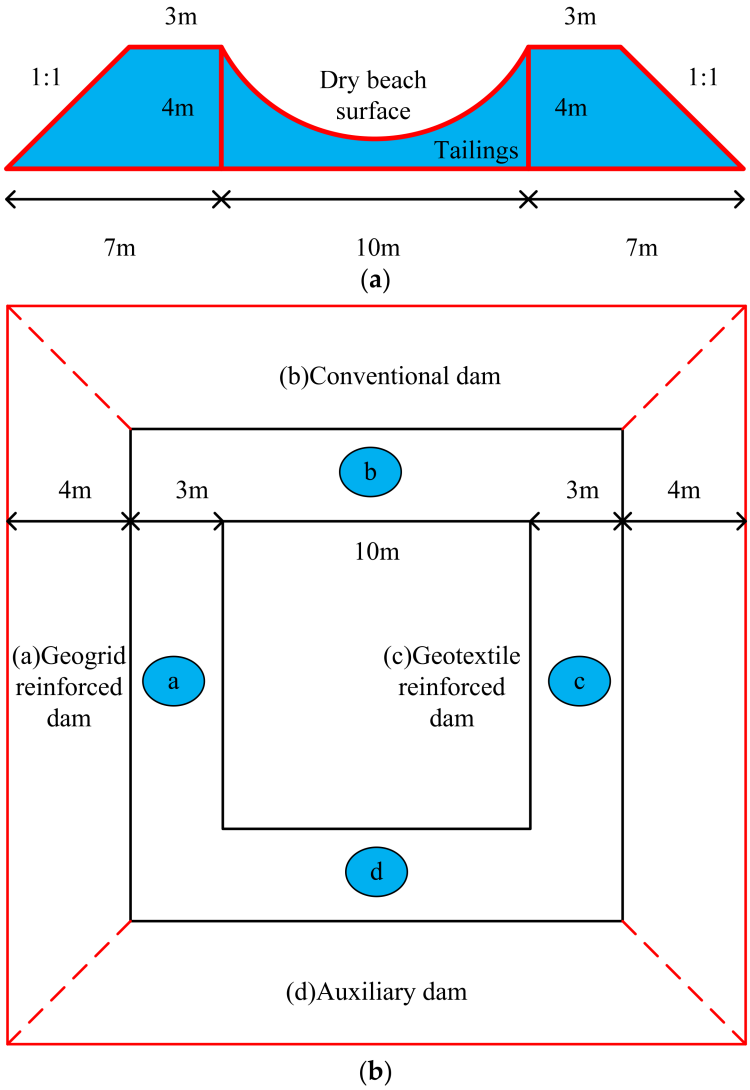

Figure 2. Design of the surrounding tailings accumulation dams. (**a**) Main and side views. (**b**) Top view.

Table 1. Stacking type and relevant parameters of surrounding dams.

Accumulation Dam	(a)	(b)	(c)
Stacking type	TGSG35 Fibreglass geogrid	Conventional dam	Needle-short fibre geotextile
Laying length	Full shop	—	Full shop
Lay spacing	1 m	—	1 m

The accumulation dam (b) was built using a conventional upstream dam-building method; the accumulation dams (a) and (c) were constructed with reinforced geosynthetics similar to the conventional dam (b), but with an additional process in which geosynthetics were laid as required in the accumulation process, namely, short-fibre needled geotextile and EGA30 glass fibre geogrid. The parameters of these two reinforcement materials are listed in Table 2. In the case of the on-site reinforced accumulation dam, the structural form was external folding.

Table 2. Performance parameters of geosynthetics.

Mechanical Parameters of Short-Fibre Needled Geotextile	Performance Index	EGA30 Geogrid Mechanical Parameters		Performance Index
Crosslateral fracture strength (kN/m)	30	Network hole size, length × width (mm)		12.7 × 12.7
Horizontal lateral nominal elongation (%)	40–80	Break strength (kN/m)	Radial	30
Min. CBR top power (kN)	13		Broadwise	30
Min. Croally power (kN)	12	Min. fault	Radial	4
Equivalent aperture (mm)	0.05–0.2	elongation(%)	Broadwise	4
Vertical permeation factor (cm/s)	1.0×10^{-3}	Min. temperature resistance (°C)		−100–280
Thickness (mm)	4.2	Thickness (mm)		2.5

2.2. Layout of the Measuring Instruments

Measuring instruments were arranged during the construction of the accumulation dams, including a PWP measuring instrument (PWP gauge) and a dam IP measuring instrument (earth pressure box). Six PWP gauges (two horizontally arranged at an interval of 2 m in the middle section of each accumulation dam) and six pressure boxes (one in the horizontal direction and one in the vertical direction of the middle cross-section of each accumulation dam) were arranged as illustrated in Figure 3. After the instrument layout was completed, all measuring instruments were connected to the data acquisition instrument and computer for field testing.

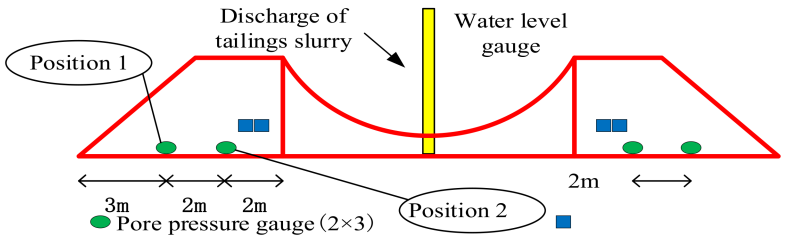

Figure 3. Layout of the field measuring instruments.

A JTM-Y3000 PWP sensor and TM-Y2000 foil micropressure box (Changzhou Jin Civil Engineering Instrument Co., Ltd., Changzhou, China) were selected as the field measuring instruments. See Table 3 for specific instrument parameters.

Table 3. Main technical parameters of the field measuring instruments.

Measuring Apparatus	Diameter × Thickness (mm)	Scale (MPa)	Sensitivity (mV/MPa)	Mode of Connection	Waterproof Performance
JTM-Y3000 pore pressure gauge	35 × 60	0.1	0.2	Full bridge	Can work in a saturated water medium
TM-Y2000 soil pressure box	117 × 30	1	Approximately 1.5		

3. Field Test Procedure

3.1. Laying Work

3.1.1. Reinforcement Layout

The geogrid and geotextile was divided into four layers; the first layer was laid at the bottom of the accumulation dam, and the second, third, and fourth layers were laid at intervals of 1 m. No reinforcement was laid on the top surface. The reinforcement layout is illustrated in Figure 4.

(**a**) (**b**)

Figure 4. Laying of reinforcement materials for the reinforced dam: (**a**) geogrid; (**b**) geotextile.

3.1.2. Sensor Embedding

Two PVC pipes were horizontally embedded in the middle section of the lowest part of the dam body of each accumulation dam (when the first layer of reinforcement material was laid for the reinforced dam). The bottom of the PVC pipe was treated with a flower tube, and both ends of the PVC pipe were wrapped with a window screen. A PWP gauge was installed in the PVC pipe at a vertical interval of 2 m from the direction of the reservoir. During the construction of the accumulation dam, in the middle of the second layer of the dam body of the first three accumulation dams (when the second layer of reinforcement material was laid for the reinforced dam), two earth pressure boxes were embedded in each accumulation dam; one was placed horizontally to measure the IP in the vertical direction, and the other was placed vertically to measure the IP in the horizontal direction. The embedding of the IP and PWP sensors in the dam body is shown in Figure 5.

(**a**) (**b**)

Figure 5. Sensor placement in the dam: (**a**) pressure box; (**b**) PWP gauge.

3.2. Completion of the Accumulation Dams

As shown in Figure 6a, a water-level gauge was inserted into the surrounding accumulation dam reservoir. As shown in Figure 6b, after the accumulation dam structure was completed, the beach surface in the reservoir was regarded as the starting point of the water level (the beach surface was approximately 1 m away from the lowest surface in the reservoir) for measuring the water level change when discharging the tailings slurry. The sensors inside each dam body were connected to the acquisition instrument and computer, which began data acquisition when the tailings slurry was discharged into the surrounding tailings accumulation dam.

(**a**) (**b**)

Figure 6. Completion of the overall piling of the reinforced tailings dam and data collection: (**a**) test dam; (**b**) water level observation.

3.3. Slurry Discharge

A tail ore slurry discharge pipe was introduced from the main slurry discharge pipe of the tailings pond to the tailings pond built on site, and the tail ore slurry was discharged into the test pond at a flow rate of approximately 100 m^3/h. During this time, the change in water level in the reservoir was observed and recorded; after 3 h of slurry discharge, the designated water level was reached, and the tailings slurry discharge was stopped. Measurement data continued to be recorded until dam breakage occurred.

At the end of data collection (approximately 18 h after slurry discharge), cracks of varying degrees occurred near the dam crest on the inner side of each test dam. The degree of cracking of the conventional dam was the most serious, and fault cracks were clearly observed (Figure 7b). Both the geogrid and geotextile dams were observed to have long cracks along the strike direction of the dam body (Figure 7a,c). The failure of the geotextile dam was significant, but neither the geotextile nor geogrid dams exhibited fault cracks.

(**a**) (**b**) (**c**)

Figure 7. Failure details of each test dam after 18 h of data collection: (**a**) geogrid-reinforced dam, (**b**) conventional dam, and (**c**) geotextile-reinforced dam.

4. Field Measurement Data Analysis

After grouting was started in the test, the variation law of the water level in the reservoir was observed over time through a water level gauge, and the change law of PWP and IP in the dam body was monitored by previously set sensors in each test dam. The test data were then compared and analysed.

4.1. Water Level Analysis in the Dam Body Reservoir

As described in the previous section, the tailings slurry was discharged into the surrounding tailings accumulation dam through the slurry discharge pipe of the tailings pond at a discharge flow rate of approximately 100 m^3/h. After the designated water level of approximately 2.5 m was reached, it was approximately 3.5 m from the lowest surface of the dam body. After the slurry discharge was stopped, the water level in the reservoir was observed until it became stable. The water level change in the surrounding accumulation dam over time is shown in Figure 8.

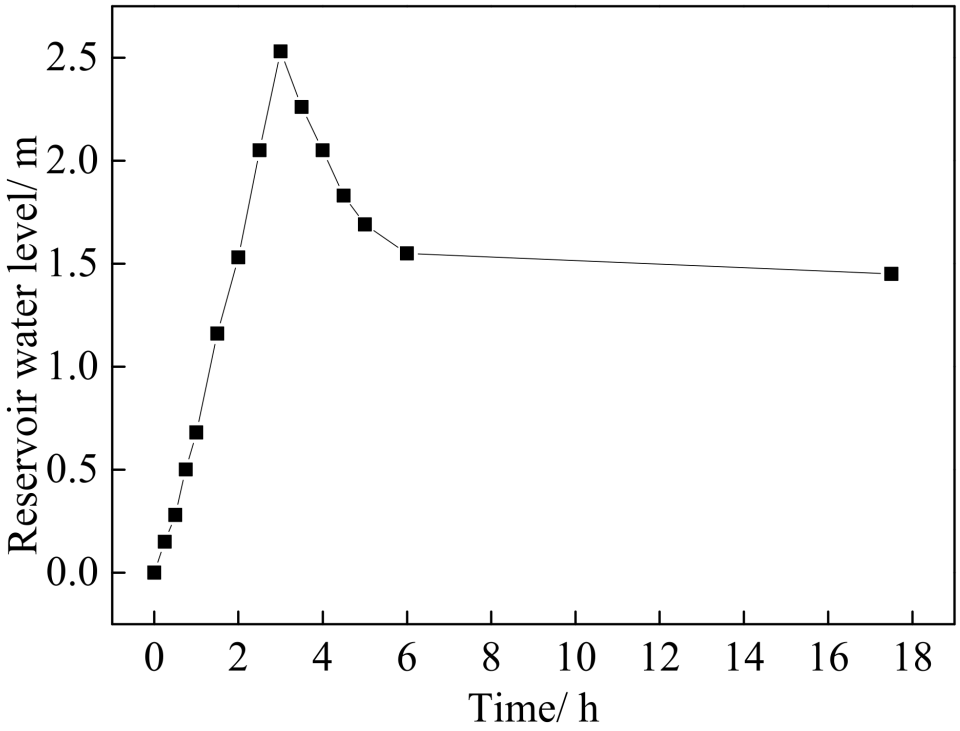

Figure 8. Relationship between reservoir water level and time.

Figure 8 shows that the water level in the reservoir increased linearly over time during the first 3 h of slurry discharge. At this stage, the tailings slurry discharge velocity was much greater than the penetration velocity of the slurry to the surrounding test dam. During the 3–6 h period, the water level in the reservoir gradually decreased over time. At this stage, the slurry was fully discharged and infiltrated into the surrounding test dam; at 6–17.5 h, the water level in the reservoir began to stabilise, indicating that the penetration of the tail ore slurry into the surrounding accumulation dams was eventually completed. Different degrees of cracking were observed near the dam crest on the inner side of each test dam after data collection.

4.2. Vertical Pressure Analysis Inside the Dam Body

4.2.1. Variation Law of IP at Different Dam Body Positions

After grouting to the surrounding tailings dam, the variation of the IP over time in the three types of test dams was analysed, as shown in Figure 9. The IP changes in the three test dams with time were essentially the same. The IP in the vertical and horizontal directions increased with time and finally stabilised. The horizontal pressure was approximately 0.4 times the vertical pressure.

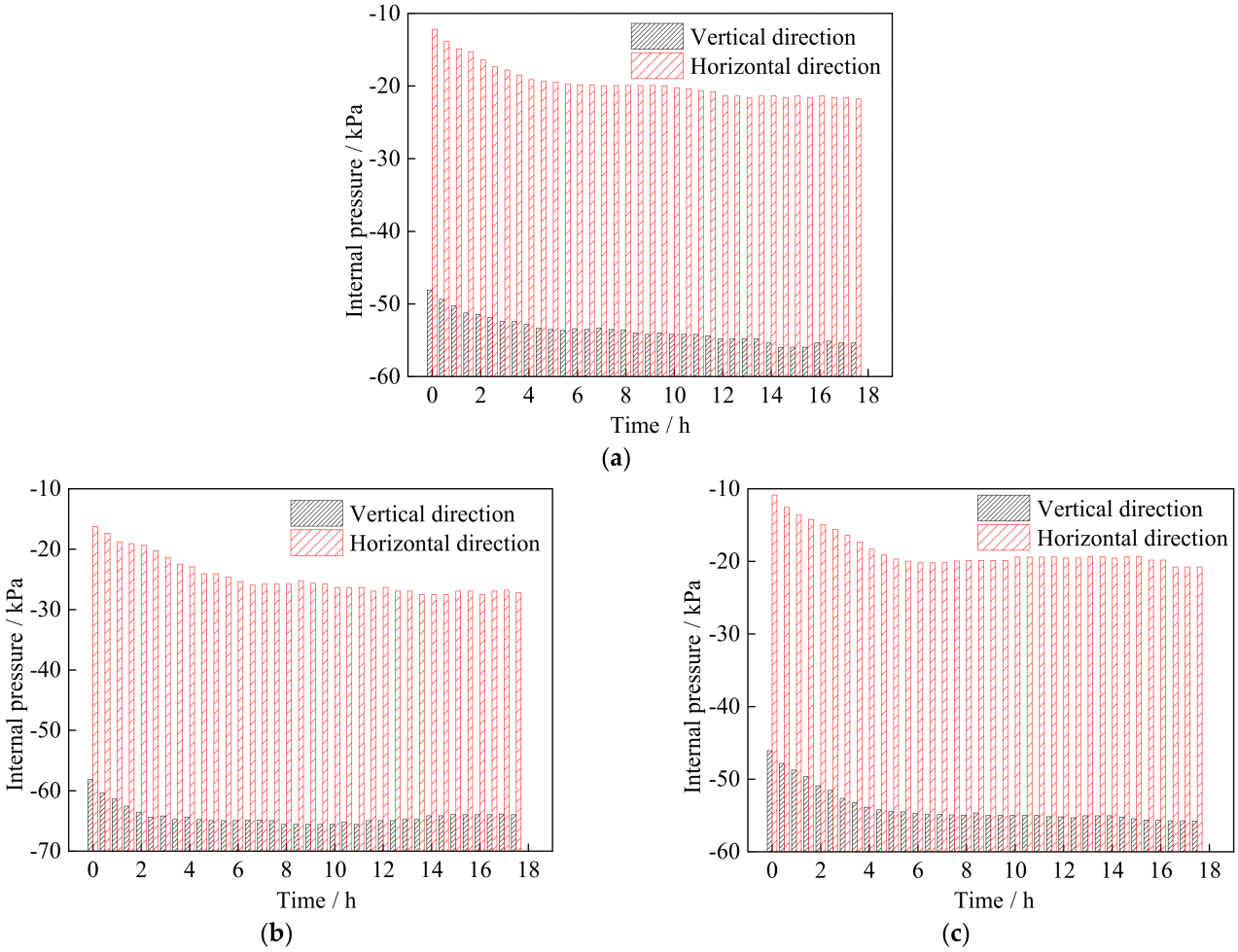

Figure 9. Relationship between pressure in the dam body and time: (**a**) geogrid-reinforced dam, (**b**) conventional dam, and (**c**) geotextile-reinforced dam.

Figure 10 shows the static earth pressure coefficient K_0 calculated according to the measured pressures in the vertical and horizontal directions for the three types of accumulation dams. K_0 increased over time until finally stabilised; the K_0 stability value of the conventional dam was 0.43, and those of the geogrid-reinforced and geotextile-reinforced dams were 0.39 and 0.37, respectively. The K_0 stability value of the reinforced tailings dams was approximately 10% lower than that of the conventional dam, indicating that reinforcement can significantly adjust the IP change of the dam body. The reinforcement can transform the IP of the dam body into tensile stress on the reinforcement material through interface friction; this limits the deformation of the tailings, thereby improving the shear strength of the tailings dam and the stability of the entire structure. Therefore, reinforcement can significantly reduce vertical pressure in the dam body.

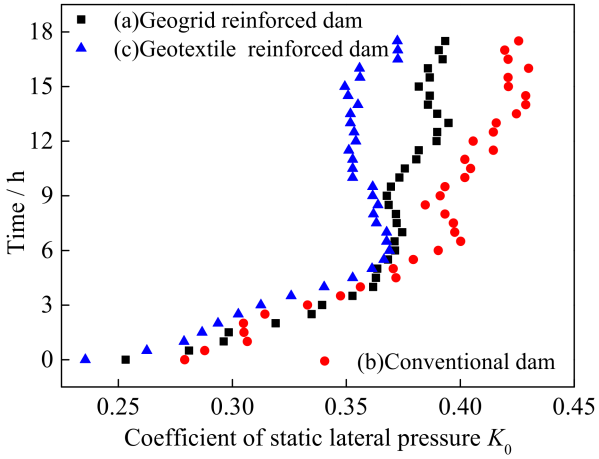

Figure 10. Relationship between the static-side pressure coefficient and time.

4.2.2. Comparative Analysis of the IP of the Tailings Accumulation Dams

Figure 11 shows a comparison of the IP of the three types of accumulation dams over time. The IP of the dam body in both vertical and horizontal directions of the three types of accumulation dams changed noticeably approximately 6 h before the observation and data measurement (4 h after the end of grouting), and then tended to be stable; however, the difference between them is that the horizontal pressure changed more sharply than the vertical pressure before stabilising. The IP of the conventional dam was quite different from that of the reinforced dams, indicating that reinforcement can effectively reduce the IP of the dam body.

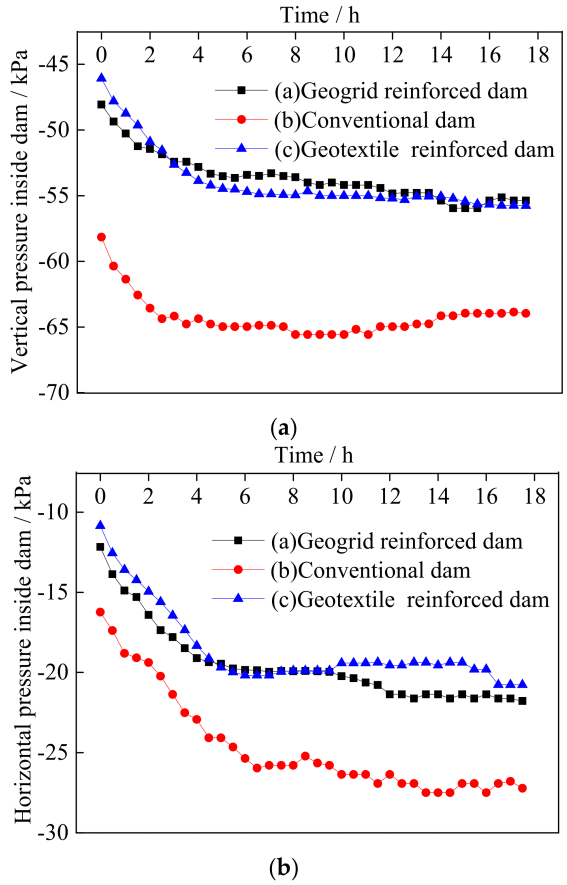

Figure 11. Comparison of IP over time in the three tailings dams: (**a**) vertical direction; (**b**) horizontal direction.

Through a comparative analysis of the geogrid-reinforced and geotextile-reinforced dams, it was found that the reduction in the IP by geogrid and geotextile reinforcements was essentially the same, indicating that reinforcement of the tailings dam can effectively reduce the IP of the dam body and enhance the stability of the tailings dam. The type of material that should be selected for reinforcement in the project should also be considered in combination with other factors and the needs of specific projects.

We further analysed the changes in the IP of the dam body throughout the data-measurement process (see Table 4 for specific data). The change rate of the IP in the horizontal direction of the three types of accumulation dams was greater than that in the vertical direction; that is, the change in IP in the horizontal direction was more sensitive. This is because the horizontal pressure changed more noticeably than the vertical pressure due to the migration of water in the dam during the entire data-acquisition process.

Table 4. Variation of IP in the dam body.

Value Case	(a) Geogrid-Reinforced Dam (kPa)		(b) Conventional Dam (kPa)		(c) Geotextile-Reinforced Dam (kPa)	
	Vertical	**Horizontal**	**Vertical**	**Horizontal**	**Vertical**	**Horizontal**
Initial value	−48.06	−12.17	−58.15	−16.23	−46.08	−10.85
Stable value	−55.95	−21.78	−64.97	−27.50	−55.77	−20.77
Variation rate	14.10%	44.12%	10.50%	40.98%	17.37%	47.76%

4.3. PWP Analysis in the Dam Body

4.3.1. Variation Law of PWP at Different Dam Body Positions

After grouting the surrounding tailings dam, the time-varying relationship of the PWP in the three test dams was analysed, as shown in Figure 12, and the PWP change values of the three test dams over time were essentially the same. The PWP increased gradually for 6 h before the observation and then tended to stabilise; the stable value of PWP near the outside of the three test dams was approximately 0.6 times that near the inside of the reservoir.

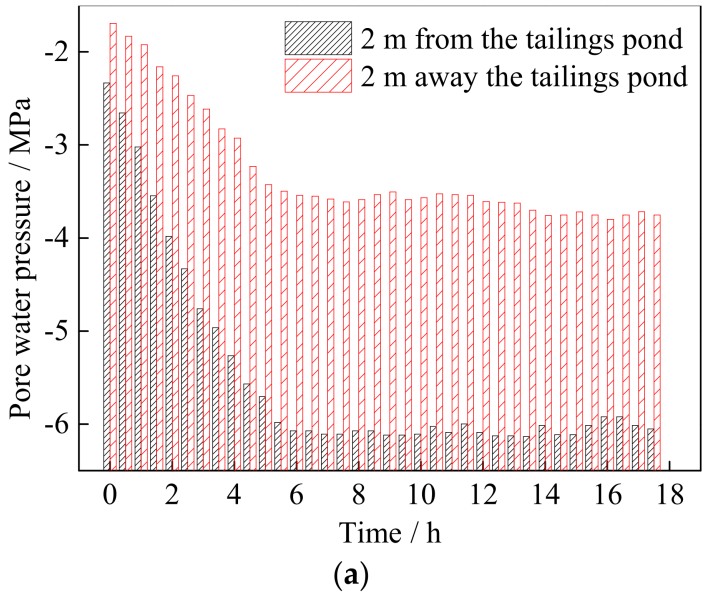

Figure 12. *Cont.*

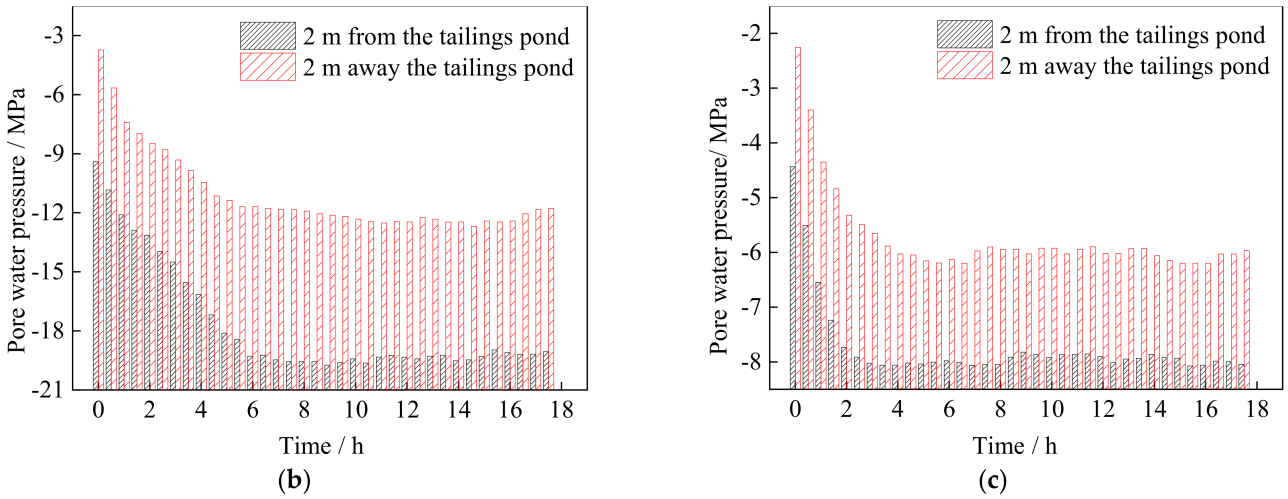

Figure 12. Relationship between PWP in the dam body and time: (**a**) geogrid-reinforced dam, (**b**) conventional dam, and (**c**) geotextile-reinforced dam.

4.3.2. Comparative Analysis of PWP at the Same Location for Different Tailings Dams

The comparison of PWP over time in the three types of accumulation dams after grouting was analysed, as shown in Figure 13. The final stable value of PWP in the conventional dam was the largest. There was little difference between the stable values of PWP in the geogrid-reinforced and geotextile-reinforced dams; moreover, the PWP stability of the two reinforced dams was much lower than that of the conventional dam, indicating that reinforcement plays a significant role in the reduction of PWP in tailings dams. Furthermore, reinforcement of tailings dams can effectively promote the reduction of the water level in the dam body because the reinforced tailings complex forms a drainage prism, both promoting the drainage of water and reducing the PWP in the dam. Through further comparative analysis of the geogrid-reinforced and geotextile-reinforced dams, it was found that the geogrid had a greater reinforcement effect on the tailings dam, which was caused by its unique mesh.

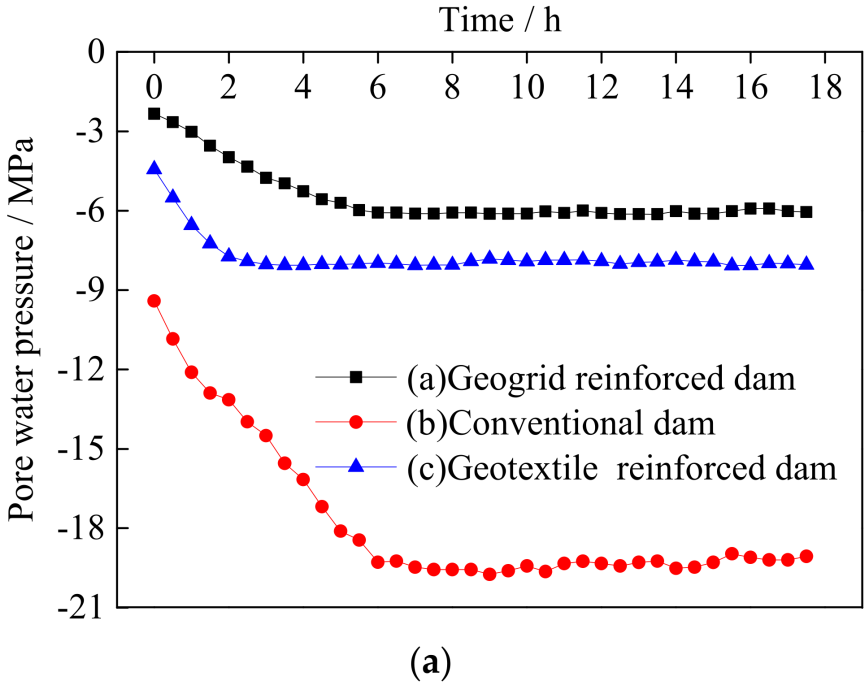

Figure 13. *Cont.*

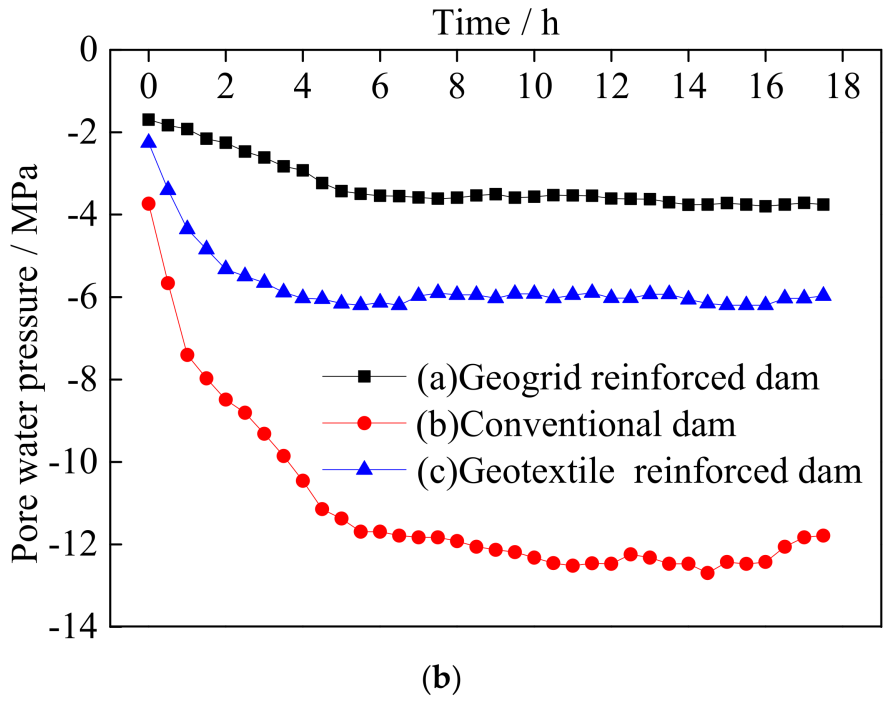

Figure 13. Comparison of PWP over time in the three tailings dams: (**a**) vertical direction; (**b**) horizontal direction.

The change in dam PWP during the entire data-measurement process was further analysed for variation (see Table 5 for specific data). Among the three accumulation dams, the change rates of PWP near and outside the reservoir of the two reinforced dams were greater than those at the two conventional dam locations, indicating that reinforcement can make the change in pore pressure inside the dam more sensitive.

Table 5. Variation of pore pressure in the dam body.

Value Case	(a) Geogrid-Reinforced Dam (kPa)		(b) Conventional Dam (kPa)		(c) Geotextile-Reinforced Dam (kPa)	
	Position 2	**Position 1**	**Position 2**	**Position 1**	**Position 2**	**Position 1**
Initial value	2.33	1.69	9.41	3.74	3.44	2.76
Stable value	6.05	3.80	19.74	12.52	8.06	6.20
Variation rate	61.48%	55.52%	47.55%	32.62%	57.32%	55.48%

4.3.3. Variation Relationship of the Saturation Line in the Dam Body

Using the PWP measurement results, the change in the final saturation line of the three test dams can be estimated, as shown in Figure 14. Reinforcement can significantly reduce the saturation line of the dam. While there is little difference between the geogrid and geotextile reinforcements in terms of the saturation line of the dam, the effect of grid reinforcement is slightly greater.

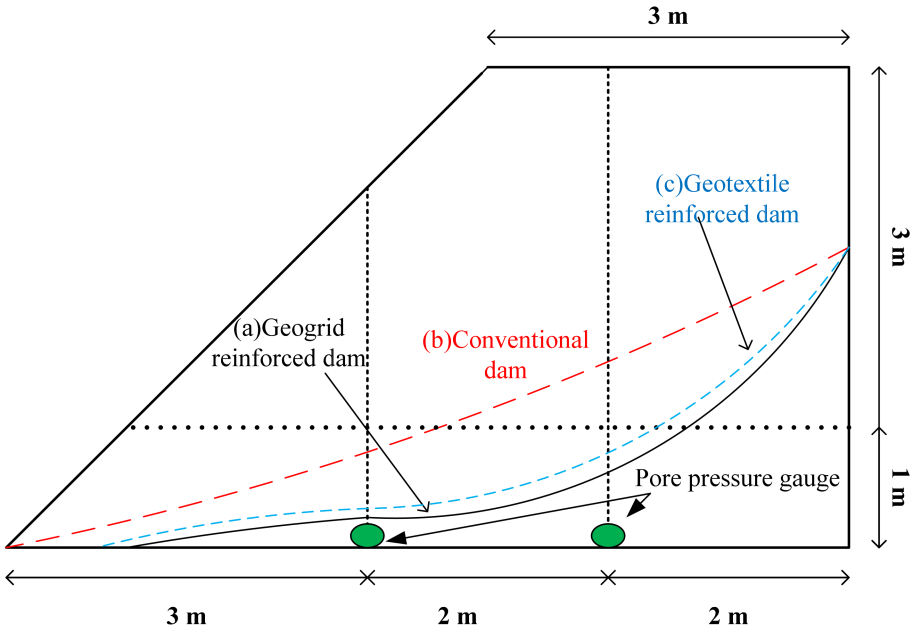

Figure 14. Schematic of the change in the final saturation line of the three test dams.

5. Conclusions

Through field prototype tests of three types of tailings accumulation dams (conventional, geogrid-reinforced, and geotextile-reinforced), this study analysed the influence of reinforcement on the tailings dams and the variation law of PWP and IP in the dam bodies after slurry discharge were analysed, and the observational data were compared and analysed. The main conclusions are as follows.

Reinforcement of tailings dams can effectively reduce the IP of dam bodies and enhance the stability of tailings dams. In terms of improving the pressure in dam bodies, the effects of geogrid and geotextile are roughly the same. Reinforcement plays a significant role in the reduction of PWP in tailings dams and can also effectively promote the reduction of the water level in the dam body. Compared with geotextiles, the geogrid had a greater overall reinforcement effect on the tailings dam due to the unique mesh of the geogrid. The type of reinforcement material that should be selected in tailings reinforcement projects should be considered in combination with other factors and specific project needs. These research results can provide a reference for the future application of geosynthetics in tailings dam design and construction.

Author Contributions: Conceptualisation, C.D. and L.L.; methodology, C.D.; software, C.D.; validation, L.L., F.Y. and B.N.; formal analysis, C.D.; investigation, L.L.; resources, C.D.; data curation, L.L.; writing—original draft preparation, C.D.; writing—review and editing, L.L.; visualisation, B.N.; supervision, C.D.; project administration, C.D.; funding acquisition, F.Y. All authors have read and agreed to the published version of the manuscript.

Funding: Research was supported by the National Natural Science Foundation of China (51774163), and the first batch of "double first class" discipline construction innovation team was funded by Liaoning Technical University (LNTU20TD-26). We appreciate the editor and anonymous reviewers' useful comments.

Institutional Review Board Statement: Not applicable.

Informed Consent Statement: Not applicable.

Data Availability Statement: All data, models, and code generated or used during the study appear in the submitted article.

Acknowledgments: The authors would like to thank the reviewers for their constructive comments that improved the paper.

Conflicts of Interest: The authors declare no conflict of interest.

References

1. Mcdermott, R.K.; Sibley, J.M. Aznalcollar tailings dam accident a case study. *Miner. Resour. Eng.* **2000**, *9*, 101–118. [CrossRef]
2. Marcus, W.A.; Meyer, G.A.; Nimmo, D.R. Geomorphic control of persistent mine impacts in a Yellowstone Park streamand implications for the recovery of fluvial systems. *Geology* **2001**, *29*, 355–358. [CrossRef]
3. Fourie, A.B.; Blight, G.E.; Papageorgiou, G. Static liquefaction as apossible explanation for themerrie spruit tailings dam failure. *Can. Geotech. J.* **2001**, *37*, 707–719. [CrossRef]
4. Kemper, T.; Sommer, S. Estimate of heavy metal contamination in soils after a mining accident using reflectance spec-troscopy. *Environ. Sci. Technol.* **2002**, *36*, 2742–2747. [CrossRef] [PubMed]
5. Tynybekov, A.K.; Aliev, M.S. The ecological condition of Kadji-Sai uranium tailings. *Environ. Secur. Public Saf.* **2005**, *47*, 187–195. [CrossRef]
6. Iryo, T.; Rowe, R.K. On the hydraulic behavior of unsaturated nonwoven geotextiles. *Geotext. Geomembr.* **2003**, *21*, 381–404. [CrossRef]
7. Shen, L.Y.; Zhou, K.P.; Wei, Z.A.; Chen, Y.L. Research on geosynthetics in tailings dam reinforcement. *Adv. Mater. Res.* **2011**, *402*, 675–679. [CrossRef]
8. Maleki, A.; Lajevardi, S.H.; Brianon, L.; Nayeri, A.; Saba, H. Experimental study on the L-shaped anchorage capacity of the geogrid by the pullout test. *Geotext. Geomembr.* **2021**, *49*, 1046–1057. [CrossRef]
9. Bathurst, R.J.; Ezzein, F.M. Geogrid pullout load-strain behaviour and modelling using a transparent granular soil. *Geosynth. Int.* **2016**, *23*, 271–286. [CrossRef]
10. Festugato, L.; Consoli, N.C.; Fourie, A. Cyclic shear behaviour of fibre-reinforced mine tailings. *Geosynth. Int.* **2015**, *22*, 196–206. [CrossRef]
11. Wei, Z.; Yin, G.; Li, G.; Wang, J.G.; Wan, L.; Shen, L. Reinforced terraced fields method for fine tailings disposal. *Miner. Eng.* **2009**, *22*, 1053–1059. [CrossRef]
12. Yin, G.; Wei, Z.; Wang, J.G.; Wan, L.; Shen, L. Interaction characteristics of geosynthetics with fine tailings in pullout test. *Geosynth. Int.* **2008**, *15*, 428–436. [CrossRef]
13. Consoli, N.C.; Nierwinski, H.P.; Da Silva, A.P.; Sosnoski, J. Durability and strength of fiber-reinforced compacted gold tailings-cement blends. *Geotext. Geomembr.* **2017**, *45*, 98–102. [CrossRef]
14. Du, C.B.; Yi, F. Analysis of the Elastic-Plastic Theoretical Model of the Pull-Out Interface between Geosynthetics and Tailings. *Adv. Civ. Eng.* **2020**, *2020*, 1–22. [CrossRef]
15. Hancock, G.R. The use of landscape evolution models in mining rehabilitation design. *Environ. Geol.* **2004**, *46*, 578–583. [CrossRef]
16. Chen, S.C.; Feng, Z.Y.; Wang, C.; Hsu, T.Y. A large-scaletest on overtopping failure of tow artificial dams in taiwan. *Eng. Geol. Soc. Territ.* **2015**, *2*, 1177–1181. [CrossRef]
17. Zhao, Y.S.; Jing, X.F.; Zhou, X.; Cai, Z.Y.; Liu, K.H. Experimental study on blocking action of bar strip on tailings dam overtopping. *China Saf. Sci. J.* **2016**, *26*, 94–99. (In Chinese) [CrossRef]
18. Yin, G.Z.; Zhang, D.M.; Wei, Z.A. Testing study on interaction characteristics between grained tailings and geosynthetics. *Chin. J. Rock Mech. Eng.* **2004**, *23*, 426–429. (In Chinese) [CrossRef]
19. Jing, X.; Chen, Y.; Williams, D.; Serna, M.; Zheng, H. Overtopping Failure of a Reinforced Tailings Dam: Laboratory Investigation and Forecasting Model of Dam Failure. *Water* **2019**, *11*, 315. [CrossRef]
20. Matsuoka, H.; Liu, S.H. New earth reinforcement method by geotextile bag. *Soils Found.* **2003**, *43*, 173–188. [CrossRef]
21. Hatami, K.; Bathurst, R.J.; Pietro, P.D. Static response of reinforced soil retaining walls with nonuniform reinforcement. *Int. J. Geomech.* **2001**, *1*, 477–506. [CrossRef]
22. Yang, G.Q.; Lu, P.; Zhang, B.J.; Zhou, Q.Y. Research on geogrids reinfoeced siol retaining wall with concrete rigid face by field test. *Chin. J. Rock Mech. Eng.* **2007**, *26*, 2077–2083. (In Chinese)
23. Zhu, G.Q.; Wang, C.Z.; Li, X. Study of long-term performances of reinforced slope at expressway. *Rock Soil Mech.* **2012**, *33*, 3103–3108+3200. (In Chinese)